CHAPTER 6
EARLY CRETACEOUS SEAMOUNT IN MAGELLAN SEAMOUNT CHAIN

6-1. Introduction

The Fukunaga seamount at the east of the Mariana Trench in the Magellan Chain (Figure 2.1) is now dislocated by normal faulting caused by horizontal extension due to the plate subduction at the trench oceanward slope (Figure 2.8) (Ogawa *et al.*, 1994). The faulting produced many steep cliffs composed of volcanic rocks and pelagic sedimentary rocks (Figure 2.9). This seamount located at around 15° 29' N and 147° 50' E is at least 35 km in diameter and approximately 3000 m in altitude from the abyssal plain.

Two volcanic rock and four sedimentary rock samples were collected from these cliffs during the 181st dive of the JAMSTEC submersible *Shinkai 6500* on October 4th, 1993, at approximately 6016 to 6424 m depth (Figure 2.9). The collected volcanic rocks are pillow lava (sample D181-R002) and pillow breccia (sample D181-R006). Pelagic sedimentary rocks are radiolarian chert (samples D181-R001, R004 and R005) and tuffaceous radiolarian claystone (D181-R003) (Table 6.1) (Ogawa *et al.*, 1994; 1996; Ogawa and Kawata, 1998). The range of biostratigraphic age and the depth of collected rocks and the ages of the presently studied two volcanic rocks are shown in

Table 6.1. The oceanic plate beneath these sediments and rocks has the magnetic anomaly Chron M25 (Smith *et al.*, 1989; Nakanishi, 1993), which is correlated to 154 to 155 Ma according to the scale of Gradstein *et al.* (1994).

Table 6.1 Age data for rocks collected during the 181st dive. Geologic ages of sample R-001, R-003, R-004 and R-005, depth and rock's name refer to Ogawa *et al.* (1994), and absolute ages of stages refer to Gradstein *et al.* (1994).

Sample	Depth (m)	Rock	Geologic Age (Stage)	Age (Ma)	References
R-001	6424	radiolarian chert	late Valanginian-Hauterivian	134.5-127.0	Ogawa *et al.* (1994, 1996)
R-002	6361	peralkaline rhyolite	Barremian-Aptian	127.0±5.2	Hirano *et al.* (submitted)
R-003	6316	tuffaceous radiolarian claystone	early Berriasian	Ca.140.0	Matsuoka *et al.* (1997)
R-004	6284	radiolarian chert	Coniasian-Santonian	89.0-83.5	Ogawa *et al.* (1994, 1996)
R-005	6192	radiolarian chert	Cenomanian-Turonian	98.9-89.0	Ogawa *et al.* (1994, 1996)
R-006	6035	alkali olivine basalt	Danian	62.0±2.6	Hirano *et al.* (submitted)

6-2. Results

Petrography

D181-R002 was sampled at approximately 6170 m depth from a continuous outcrop of 43 m thick pillow lava sequence with a horizontal bedding (Ogawa *et al.*, 1994) (Figure 2.9). The curvature of the trachytic structure and the foliation of vesiculation in the sample suggest that this sample is part of a pillow lava whose long diameter may range approximately over 1 m. This rock is apparently fresh, gray-white in color, and is composed of abundant sanidine ($Or_{45-43}Ab_{55-57}$) and common quartz phenocrysts with subordinate amounts of hornblende (zoning of sodic to calcic-sodic amphibole) within an aphanitic groundmass including sanidine ($Or_{40-30}Ab_{60-70}$) and opaque minerals. Some resorptive quartz phenocrysts could be xenocrysts. Small grains of the alteration mineral zoisite occur in the groundmass, but the alteration is not very great.

D181-R003 was collected from an outcrop at approximately 6316 m depth (Ogawa *et al.*, 1994) and is a tuffaceous radiolarian claystone composed of fresh volcanic glass, clay fragments, plagioclase (An_{80-70} Ab_{20-30}), extremely well preserved radiolaria (Ogawa *et al.*, 1996; Matsuoka *et al.*, 1997; Ogawa and Kawata, 1998), foraminifera, and other tests. These minerals and tests are 0.1-0.3 mm in diameter, and tuffaceous parts may be turbidites.

D181-R006 is a pillow breccia collected from an outcrop at approximately 6035 m depth. Below this outcrop, a Quaternary thin (less than 10 m thick) pelagic clayey sediment covers the Cretaceous chert sequence (Ogawa *et al.*, 1994) (Figure 2.9). An X-ray diffraction analysis shows that R006 is composed of lower temperature

alteration minerals, such as goethite, amphibole, persettensite and illite-montmorillonite interlayered clays. Seriate texture in sanidine (Or_{100-35}) and plagioclase ($An_{75-60}Ab_{25-40}$) and relic phenocryst of olivine suggest that the original rock is an olivine-bearing alkali-basalt (called "alkali olivine basalt").

Geochemistry

Results of major and trace element compositions of bulk rocks by XRF, EPMA and LAM-ICPMS analyses show in Table 6.2 and 6.3, respectively. R002 is a very differentiated high SiO_2 alkaline rock. With more than 75 wt % SiO_2 and more than 8 wt% Na_2O+K_2O it should be called peralkaline rhyolite (Hirano *et al.*, submitted) (Figure 6.1, Table 6.2). Geochemical compositions by the microprobe data of volcanic glasses in R003 show hawaiite compositions of the Na_2O-rich alkali-basalt (Figure 6.1, Table 6.2). As mentioned above, because R006 is composed of lower temperature alteration minerals this is only described as the alkali olivine basalt (Hirano *et al.*, submitted).

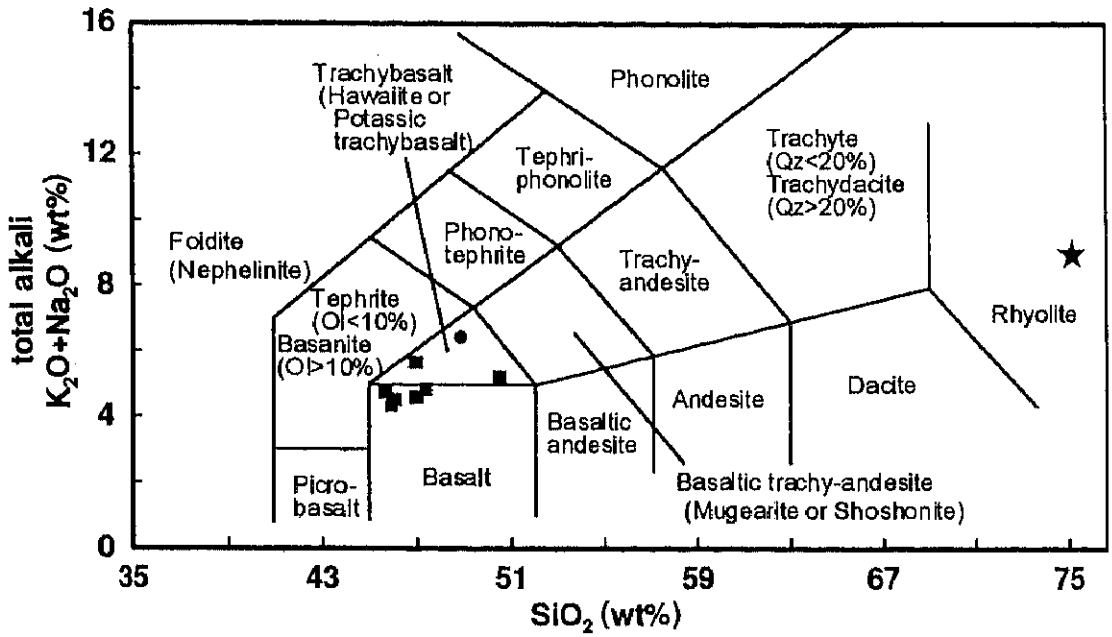

Figure 6.1 SiO_2-total alkali diagrams of D-181 R-002 (asterisk), R-003 (squares) and R-006 (circle) from Unnamed Seamount, Magellan Seamount Chain, at the Mariana Trench.

Table 6.2 Major element compositions of samples obtained by electron microprobe analysis for volcanic glasses in R-003, and by Ogawa *et al.* (1994) for the bulk compositions of R-002 and R-006.

	R-003							R-002	R-006
	Glass O	Glass J	Glass C	Glass F	Glass G	Glass H	Glass A	Bulk*	Bulk*
method	EPMA	EPMA	EPMA	EPMA	EPMA	EPMA	EPMA	XRF	XRF
(wt%)									
SiO_2	46.97	45.89	50.59	45.93	47.32	45.69	47.02	75.27	48.89
TiO_2	4.55	4.57	3.18	3.46	4.46	4.66	3.32	0.17	2.52
Al_2O_3	13.67	13.07	17.48	14.41	13.61	12.59	14.34	10.78	15.86
FeO	12.48	13.44	9.36	11.10	12.75	13.91	10.99	3.44	11.83
MnO	0.24	0.19	0.17	0.22	0.12	0.25	0.17	0.05	0.08
MgO	4.33	4.90	3.02	6.34	4.44	4.98	6.09	0.07	2.17
CaO	8.72	10.32	9.21	11.90	9.86	10.72	10.79	0.12	6.09
Na_2O	4.19	3.47	4.12	3.37	3.44	3.54	3.75	4.65	3.01
K_2O	1.37	0.95	1.00	0.87	1.25	1.10	0.76	4.33	3.37
Cr_2O_3	0.00	0.02	0.00	0.02	0.03	0.07	0.00	-	-
V_2O_3	0.32	0.38	0.25	0.23	0.26	0.19	0.20	-	-
NiO	0.00	0.01	0.00	0.00	0.00	0.07	0.00	-	-
P_2O_5	0.88	0.60	0.65	0.46	0.69	0.63	0.41	0.03	1.93
LOI	-	-	-	-	-	-	-	0.59	3.80
Total	97.71	97.80	99.03	98.29	98.21	98.38	97.84	99.53	99.57

* From Ogawa *et al.* (1994), XRF analysis by Dr. D. James, University of Edinburgh

Table 6.3 Trace element compositions of samples obtained by LAM ICP-MS analysis for volcanic glasses in R-003, and by Ogawa *et al.* (1994) for the bulk compositions of R-002 and R-006.

	R-003							R-002	R-006
	Glass O	Glass J	Glass F	Glass G	Glass H	Glass A	Glass A	Bulk*	Bulk*
method	ICP-MS	ICP-MS	ICP-MS	ICP-MS	ICP-MS	ICP-MS	ICP-MS	XRF	XRF
(ppm)									
Sc	-	-	-	-	-	-	-	0.0	32.5
V	15.46	31.80	36.94	23.54	22.65	28.56	105.66	8.3	144.0
Cr	-	-	-	-	-	-	-	10.4	238.6
Ni	-	-	-	-	-	-	-	5.9	73.4
Cu	-	-	-	-	-	-	-	2.9	88.6
Zn	-	-	-	-	-	-	-	277.8	168.5
Rb	28.79	32.58	42.77	32.55	35.90	33.94	39.57	137.4	56.6
Sr	76.15	102.11	134.11	83.12	94.48	145.80	182.20	11.7	363.6
Y	2.99	4.17	4.85	3.11	3.78	4.62	6.67	192.2	47.4
Zr	38.78	56.77	64.79	41.92	53.63	56.67	77.65	1471.1	188.2
Nb	2.64	4.92	5.62	2.41	3.49	6.29	13.99	186.8	41.3
Ba	189.34	233.80	264.33	210.39	221.10	235.11	226.40	72.6	196.1
La	3.99	5.55	6.45	3.67	4.66	6.49	10.44	79.0	41.3
Ce	8.72	11.63	13.81	7.89	9.93	15.49	23.71	234.1	67.7
Pr	0.95	1.59	1.57	0.86	1.03	1.63	3.10	-	-
Nd	3.47	6.26	5.65	2.44	3.49	5.44	12.00	112.3	49.4
Sm	0.55	3.00	4.20	0.72	0.92	1.08	3.00	-	-
Eu	0.20	0.94	0.78	0.29	0.17	0.41	0.86	-	-
Gd	0.47	2.76	3.11	0.66	0.66	1.33	3.30	-	-
Tb	0.10	0.44	0.37	0.10	0.10	0.17	0.37	-	-
Dy	0.63	2.43	1.78	0.69	0.78	0.81	2.94	-	-
Ho	0.13	0.55	0.44	0.11	0.11	0.21	0.46	-	-
Er	0.29	2.69	2.23	0.71	0.42	0.52	2.50	-	-
Tm	0.06	0.48	0.41	0.12	0.10	0.08	0.37	-	-
Yb	0.47	3.55	2.51	0.62	0.54	0.55	2.61	-	-
Lu	0.06	0.40	0.40	0.13	0.12	0.09	0.42	-	-
Hf	0.97	2.60	2.35	1.72	1.72	1.89	2.88	-	-
Ta	0.15	0.68	0.67	0.23	0.31	0.39	0.80	-	-
Pb	8.78	15.15	12.90	9.92	7.94	8.64	13.70	12.3	3.4
Th	0.97	0.92	1.52	1.23	1.18	1.34	1.79	20.4	4.3
U	0.74	0.57	1.11	0.85	0.73	0.86	0.87	-	-

* From Ogawa *et al.* (1994), XRF analysis by Dr. D. James, University of Edinburgh

Ar-Ar Age

For sample D181-R002, alkali-feldspar phenocrysts were separated from groudmass, and for sample D181-R006, pieces of whole rock a few mm in size were analyzed by the ^{40}Ar-^{39}Ar method. The data and results can be obtained in Table 6.3 (Hirano *et al.*, submitted).

In the case of D181-R002, we can not consider 127.0±5.2 Ma in Figure 6.2 as a plateau age, because it was not obtained over three fractions. However, the two fractions (1200 and 1300 °C) cover more than 80 % cumulative ^{39}Ar, and we consider the age to be geologically reliable. In the $^{36}Ar/^{40}Ar$ - $^{39}Ar/^{40}Ar$ diagram of R-002 (Figure 6.2), on the other hand, the data do not tightly fit on this line.

For D181-R006 the data points scatter irregularly in the $^{36}Ar/^{40}Ar$-$^{39}Ar/^{40}Ar$ diagram (Figure 6.2), but if we omit the three lowest temperature fractions (600, 800 and 900 °C) from the calculation, because the isotope compositions in these fractions seem to be disturbed by alteration, we obtain a well-defined isochron (Figure 6.2). The age spectrum (Figure 6.2) shows a plateau age of 62.0±2.6 Ma, which is in accordance with the three middle temperature fractions in 95 % confidence level.

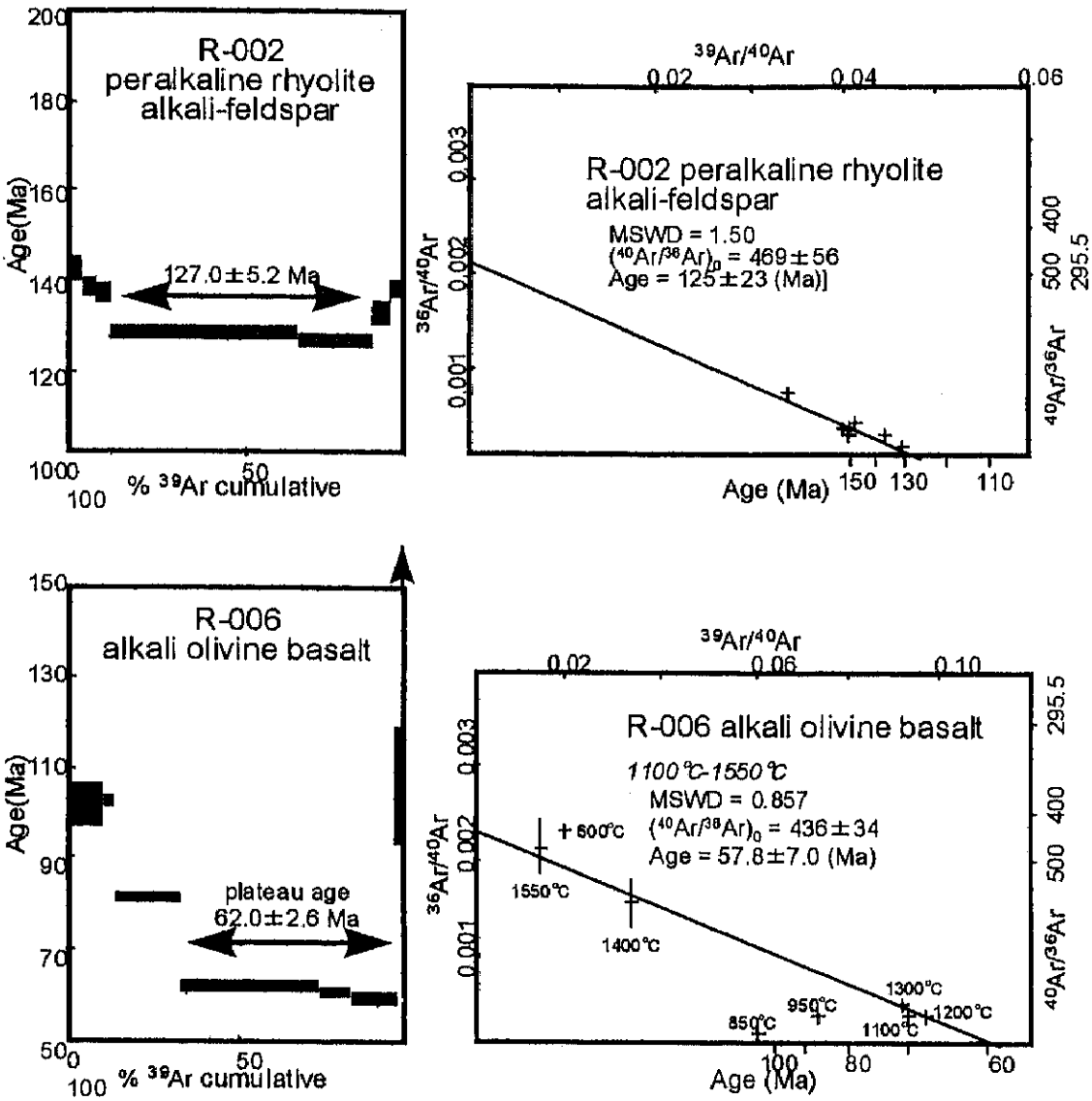

Figure 6.2 Age spectra and isochron diagrams for $^{40}Ar/^{39}Ar$ incremental heating experiments on alkali-feldspar phenocrysts in the R-002 peralkaline rhyolite (a) and on the R-006 alkali olivine basalt (b). We used different J value for each sample; (a) $J=(3.64 \pm 0.15) \times 10^{-3}$ and (b) $J=(3.49 \pm 0.14) \times 10^{-3}$, which define a dimensionless parameter determined for each irradiation from standard samples whose ages are known from conventional potassium-argon measurements (Mitchell, 1968). Standard samples are Bern4B (17.1±0.5 Ma) and a couple of HD-B1 biotite (24.0±0.4 Ma). The correction factors for the interfering isotopes during the irradiation of samples were determined experimentally as follows; $(^{36}Ar/^{37}Ar)_{Ca}=(3.70 \pm 0.22) \times 10^{-4}$, $(^{39}Ar/^{37}Ar)_{Ca}=(12.06 \pm 0.35) \times 10^{-4}$ and $(^{40}Ar/^{39}Ar)_{K}=(3.24 \pm 0.89) \times 10^{-2}$. The mean squared weighted deviations, MSWD=SUMS/(n-2) (York, 1969), indicates how well data fit the least-squares calculated straight line.

6-3. Discussions

Formation History of Unnamed Seamount

The rocks were successively collected from the lower part of the cliffs as R-001, R-002 and so on, but, according to the combination of ^{40}Ar-^{39}Ar ages and fossil ages, the samples are not in correct stratigraphic order from the lower to the upper (Table 6.1). Ogawa *et al.* (1994, 1996) interpreted that some normal faults may have disturbed the stratal disposition (Figure 2.9).

Using these volcanic ages and other sedimentary rock ages, we can illustrate the formation history of this seamount as follows (Figure 6.3):

① Generation of the oceanic plate at 155-154 Ma.

② The radiolarian pelagic sediments (R-003 and R-001) were deposited at around 140 Ma and 135-124 Ma, respectively, with an intermission of seamount volcanic activities (the first activity; R-003) of hawaiite. Hawaiite is thought to be characteristic of the main shield volcanic activity in common seamounts (Macdonald and Katsura, 1964).

③ The last volcanic activity of the main stage of this seamount is represented by R-002, a very differentiated alkaline rock (peralkaline rhyolite) commonly erupted at the last stage of the main shield volcanism like Hawaii (Macdonald and Katsura, 1964; Nakamura, 1986).

④ Then, the volcanic edifice was covered with pelagic sediments (R-004 and R-005) during the Late Cretaceous, Coniasian-Santonian and Cenomanian-Turinian, respectively (Ogawa *et al.*, 1994).

⑤ Finally, during the Danian, early in the Paleocene, volcanism resumed and the pillow breccia of R-006 was erupted.

Long Life of Volcanic Activity

The age of R-003, the oldest seamount activity, Berriasian (approximately 140 Ma) (Matsuoka *et al.*, 1997), is 8-18 m.y. older than that of R-002. Thus the main shield volcanic period (approximately 8 to 18 m.y.) calculated from the ages between R-003 and R-002 is much longer than the Hawaiian shield volcanic period (a few m.y.; Macdonald and Katsura, 1964; Nakamura, 1986). Such a long period of main shield volcanism suggests that this seamount remained at a hotspot for a long time. The reason may be attributed to either of the following two possibilities:

- An abundant heat supply as in the superplume episode in the Early Cretaceous (Cox, 1991; Larson, 1991; Larson and Kincaid, 1996)
- The absolute motion of the Early Cretaceous Pacific Plate on a fixed hotspot was very slow in contrast to the present fast motion.

The latter reason is actually reported as absolute Pacific Plate motions in Early Cretaceous by Duncan and Clague (1985) and Henderson *et al.* (1984), whose rates are 3 to 6 cm/yr. Hotspot on the slow spreading plate is similar to the present setting of the Canarian hotspot in the middle Atlantic Ocean, where the volcanism from the main shield basaltic to the late stage differentiated lavas has continued for as long as approximately 20 m.y. after the Miocene (Freundt and Schmincke, 1995), being

attributed to the slow moving Atlantic ocean floor (a few cm/yr; Jackson & Reid, 1983) (Figure 6.4).

Seamount Rejuvenation at Paleocene

The very long time span between R-002 and R-006 (over 60 m.y.) for one series of seamount volcanism, on the other hand, clearly suggests that this seamount has undergone at least two independent periods of volcanism in the Early Cretaceous and Paleocene periods, respectively. Rejuvenation of this Early Cretaceous seamount in the Paleocene may have resulted from reheating of this seamount by the passage of another hotspot (Figure 6.3).

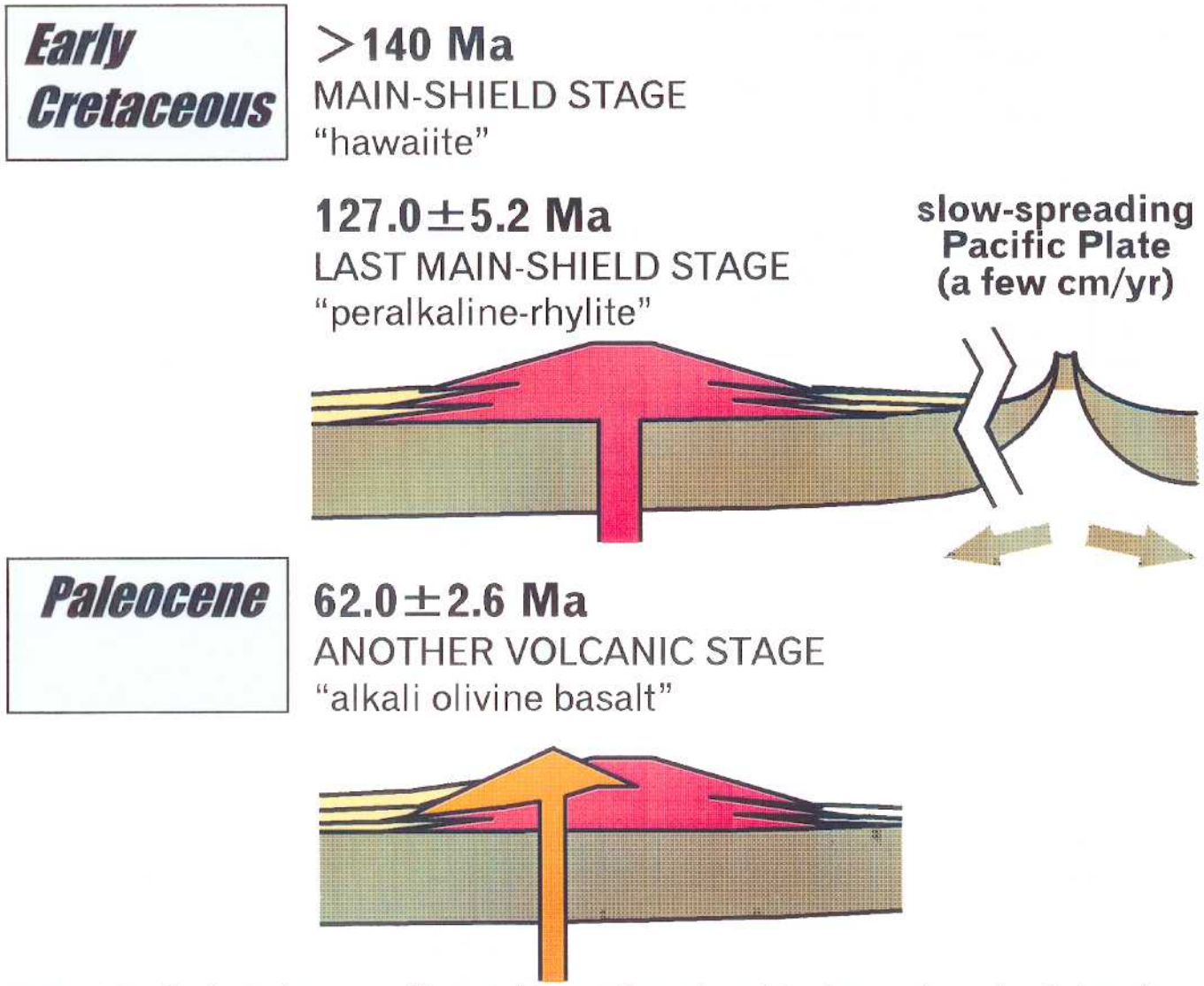

Figure 6.3 Geologic phenomena illustrated from radiometric and fossil ages of samples. Referred to Gradstein et al. (1994) and Harland et al. (1982) for time scale, Matsuoka et al. (1997) and Ogawa et al. (1994, 1996) for age duration of samples.

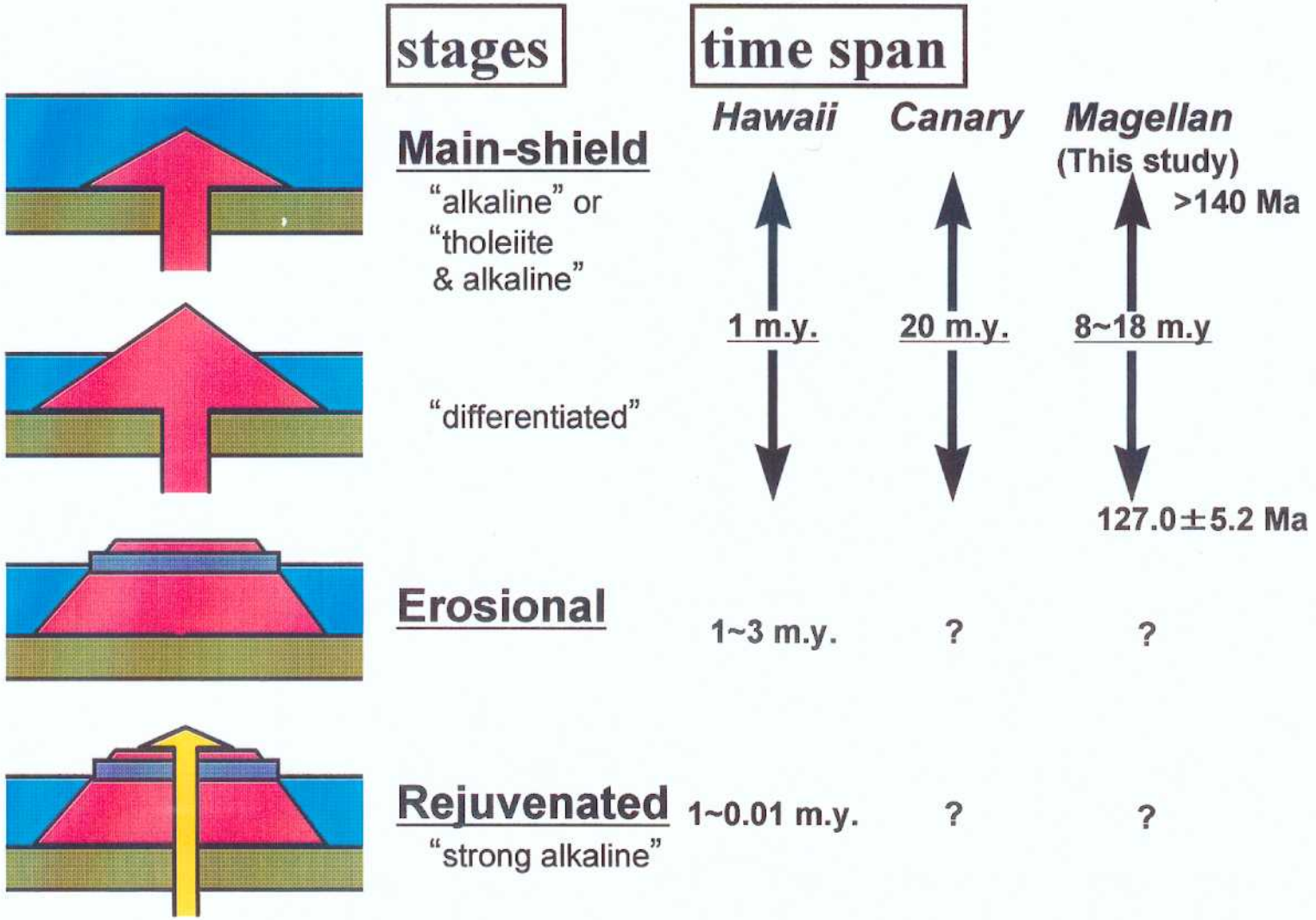

Figure 6.4 Sequence of oceanic island volcanic activity. Unnamed Seamount in this study and the Canary hotspot are longer life of volcanism than Hawaiian volcanism.